

**GSA Data Repository item 2017070. Analytical methods, geologic map, monazite and zircon U-Pb Concordia plots, monazite elemental (x-ray) maps, zircon and monazite data tables, whole rock data table, and monazite standards results**

Appendix DR1. Analytical methods

Figure DR1. Geologic map

Figure DR2. U-Pb Concordia plot for zircon

Figure DR3. U-Pb Tera-Wasserburg plot for monazite

Figure DR4. Elemental maps of monazite

Figure DR5 LASS Sm-Nd + U-Pb isotope data for monazite reference materials

Table DR1. LASS Sm-Nd + U-Pb isotope data for monazite grains A, B, and C

Table DR2. Lu-Hf and U-Pb isotope data for zircon

Table DR3. Whole rock geochemical and isotope data

Table DR4. LASS Sm-Nd and U-Pb isotope data for monazite reference materials

## **Appendix DR1. Sample processing and imaging; U-Pb analytical methods; Sm-Nd-REE analytical methods; whole rock Sm-Nd isotope analytical methods.**

### **Sample processing and imaging**

Accessory minerals were separated from each sample using standard crushing, heavy liquid, magnetic separation, and hand-picking techniques. The mineral grains were mounted in epoxy and polished to reveal their interiors. The internal zoning was then documented using back-scattered electron (BSE) imaging for monazite, and cathodoluminescence (CL) using a Jeol JXA-8230 SuperProbe at Memorial University of Newfoundland.

X-ray maps were made on selected monazite grains (e.g., grains 2, 20, and 21) using the same Jeol JXA-8230 SuperProbe. The conditions used were 15 kV, 250 nA, W filament, with a focussed beam. The step size for the X-ray maps was 0.76 µm x 0.76 µm with a dwell time of 200 ms per step. The acquisition time for the X-ray maps ranged between 9 and 12 hours. The X-ray maps were processed using the Jeol software.

### **LASS analytical methods-monazite**

Monazite from the peraluminous granite sample SW-1 was analyzed using the Laser Ablation-Split Stream (LASS) method at Memeorial Universtiy of Newfoundland. The main methodology, instrument specifics, and reference material specifics are described in detail in Goudie et al. (2014) and Fisher et al. (2011a), and thus only a few details relevant to the present study are given here. This method involved the ablation of

sample and standards using a 20μm laser beam (80μm beam for LREE glass standard) operated at 6Hz and 6 J/cm<sup>2</sup>. The ablation aerosol was split downstream of the laser cell to direct a portion of the ablated material to a ThermoFinnigan Element2 ICPMS for measurement of U-Th-Pb isotope measurement and to ThermoFinnigan Neptune MC-ICPMS for measurement of Sm-Nd isotope composition (in addition to isotopes of Ce, Eu, and Gd for concentration determination). Results of quality control standard Mae Klang monazite are presented below. Additionally, the REE elemental ratios of Trebillock monazite, which are treated as unknowns here, are also presented.

### **U-Pb analytical methods-monazite**

As discussed in detail in Goudie et al. (2014), the U-Th-Pb isotope composition (age) of unknowns was calibrated to the Trebilcock monazite standard, which was also used as the calibration material for <sup>143</sup>Nd/<sup>144</sup>Nd. Data for both U-Th-Pb and Sm-Nd-REE analyses were processed using the Iolite software package (Paton et. al., (2010, 2011)).

The Sm-Nd-REE Iolite Data Reduction Scheme is available from the first author.

### **Sm-Nd-REE analytical methods**

<sup>143</sup>Nd/<sup>144</sup>Nd -Due to the reported bias of LA-MC-ICPMS determinations of Nd isotope composition relative to those obtained by thermal ionization mass spectrometry (TIMS), the benchmark technique for Sm-Nd isotope analysis, the reported <sup>143</sup>Nd/<sup>144</sup>Nd presented here is normalized based on interspersed analyses of mineral reference materials (in this case Trebilcock monazite) which have been previously characterized by

replicate TIMS analyses (see Fisher et al., 2011a). The magnitude of this correction is typically less than 0.5 epsilon units. The  $^{143}\text{Nd}/^{144}\text{Nd}$  results of standard analyses are given in table DR4 below and plotted in Fig. DR5. Normalization is based on the mean of the measured laser ablation analyses according to equation 1:

$$\text{Sample}_{corr} = \text{Sample}_{meas} * \left( \frac{\text{Std}_{true}}{\text{Std}_{meas}^{mean}} \right) \quad \text{Eqn. 1}$$

$^{147}\text{Sm}/^{144}\text{Nd}$ -Correction of the measured  $^{147}\text{Sm}/^{144}\text{Nd}$  is described in detail in Fisher et al. (2011a), and is corroborated by the close agreement between the  $^{147}\text{Sm}/^{144}\text{Nd}$  determined for reference minerals during the course of this study and those determined by ID-TIMS for the same material. Due to the ubiquitous Sm/Nd zoning present in natural minerals, and the difficulty in producing synthetic mineral standards with homogeneous Sm/Nd, quantification of the accuracy and precision of LA-MC-ICPMS measurement of  $^{147}\text{Sm}/^{144}\text{Nd}$  is difficult. The Trebilcock monazite standard has a relatively restricted range in Sm/Nd, and thus offers a good estimate of the reproducibility of our Sm/Nd measurements (see Fisher et al., 2011a). The  $^{147}\text{Sm}/^{144}\text{Nd}$  measured for the Trebilcock standard during the course of this study is  $0.2242 \pm 0.0058$  (2SD) which is in agreement with measured TIMS values ( $0.2167 \pm 0.0125$ ) and attests to the accuracy of the technique, though the measured values during this study are consistently on the higher end of the TIMS range. We attribute this to using a single piece of this standard with Sm/Nd slightly higher than the mean of the TIMS analyses. The relative standard deviation for Trebilcock monazite analyzed during this study is

~2.5%, which we consider to be a worse case estimate of the reproducibility of this method. As shown in figure DR5 (and Table DR4), our measurements of Trebilcock monazite display homogeneous  $^{143}\text{Nd}/^{144}\text{Nd}$  and a relatively restricted range of Sm/Nd in agreement with results from ID-TIMS analyses (Fisher et al., 2011).

**Ce/Gd and Eu/Eu\*-** A single data acquisition comprises the measurement of a number of Nd isotopes (143, 144, 145, 146) and Sm isotopes (147, 149) along with isotopes of Ce (142), Eu (153), and Gd (155). In order to determine the relative abundance of each element the signal intensity (in volts) is measured for the Ce, Eu, and Gd isotopes above as well as  $^{146}\text{Nd}$  and  $^{149}\text{Sm}$ . These voltages are then abundance normalized using the following isotopic abundances  $^{142}\text{Ce}$  (11.08%),  $^{146}\text{Nd}$  (17.19%),  $^{149}\text{Sm}$  (11.30%),  $^{153}\text{Eu}$  (52.20%), and  $^{155}\text{Gd}$  (15.65%). With the exception  $^{142}\text{Ce}$ , all other isotopes are interference-free. The isobaric interference of  $^{142}\text{Nd}$  on  $^{142}\text{Ce}$  is mathematically corrected using the measured  $^{146}\text{Nd}$  and a  $^{142}\text{Nd}/^{146}\text{Nd}$  of 1.5782 (Eqn. 2 and 3).

$$^{142}\text{Ce}(v)_{calculated} = total142(v) - ^{142}\text{Nd}(v)_{calculated} \quad \text{Eqn. 2}$$

$$^{142}\text{Nd}(v)_{calculated} = ^{146}\text{Nd}(v)_{measured} * \left( \frac{^{142}\text{Nd}}{^{146}\text{Nd}_{true}} \right) \quad \text{Eqn. 3}$$

**Ce/Gd** is determined using the resulting Ce and Gd abundance normalized REE voltages. These data are then further normalized to the LREE glass described in Fisher et al., 2011a. This normalization theoretically corrects for both instrumental drift (though drift was negligible (<1%) during the course of this study and thus normalization was

based on the mean of the standards) as well as differential ablation yields of the individual elements. The LREE glass has been characterized for its Ce (23,200 ppm) and Gd (3470 ppm) content, and therefore Ce/Gd (6.69), by solution ICPMS. Normalization is done using Eqn. 1 above .

**Eu/Eu\*** is a measure of the deviation of the actual Eu content of a material to that expected from a linear fit to neighboring REE's Sm and Gd, with each element normalized to chondritic (CN) abundances (Eqn. 4).

$$Eu / Eu^* = \frac{Eu_{CN}}{(Sm_{CN} * Gd_{CN})^{0.5}} \quad \text{Eqn. 4}$$

The chondrite normalization for the abundance normalized voltages of Sm, Eu, and Gd is done by dividing the these voltages by the chondritic concentration of these elements (all expressed in ppm) using the values of McDonough and Sun (1995). The resulting Eu/Eu\* is further normalized to the Eu/Eu\* (similarly calculated) determined in the LREE glass. Table 5 in Fisher et al. (2011a) summarizes a comparison of this approach to that of a 'typical' LA-ICPMS measurement (ie., normalized to a glass standard with further internal normalization done by electron microprobe elemental concentration analyses of a major mineral- see Jackson et al. (1992) for details). The data for each of the mineral standards analyzed during this study agree well with those of the Fisher et al. (2011a) study.

### **LASS quality control standard**

Twenty-two analyses of the Mae Klang monazite (used here as a quality control standard) yielded a mean  $^{143}\text{Nd}/^{144}\text{Nd}$  of  $0.512641 \pm 28$  (2SD) and a  $^{147}\text{Sm}/^{144}\text{Nd}$  range of 0.0867 to 0.1146, both of which are in excellent agreement with the ID-TIMS values presented by Fisher et al. (2011a) (mean  $^{143}\text{Nd}/^{144}\text{Nd} = 0.512646 \pm 10$  (2SD); range of  $^{147}\text{Sm}/^{144}\text{Nd}$  0.0870 to 0.1209). Simultaneous U-Th-Pb age determinations yielded a  $^{207}\text{Pb}$ -corrected weighted mean  $^{206}\text{Pb}/^{238}\text{U}$  age of  $26.8 \pm 0.3$  Ma ( $2\sigma$ ), and a weighted mean  $^{208}\text{Pb}/^{232}\text{Th}$  age of  $27.1 \pm 0.2$  Ma ( $2\sigma$ ), both of which are in agreement with the ID-TIMS age of  $26.8 \pm 0.5$  Ma determined by Dunning et al. (1995).

### **Whole rock Sm-Nd isotope analytical methods**

Whole rock powder for SW-1 was dissolved in Savilex<sup>©</sup> Teflon beakers using an 8 ml (4:1) mixture of 29 M HF – 15 M HNO<sub>3</sub>. Prior to acid digestion, a mixed  $^{150}\text{Nd}/^{149}\text{Sm}$  spike was added. After five days of digestion, the solution was evaporated to dryness and then taken up in a saturated solution of 6 M HCl and H<sub>3</sub>BO<sub>3</sub> (boric acid) for at least 24 hours. Addition of boric acid ensured that any remaining solid fluorides were converted to soluble chlorides (Mulcahy et al., 2009). The sample was then evaporated to dryness and re-dissolved in 2.5 M HCL. Bulk rare earth elements (REE) were then isolated using cation exchange resin AG-50W-X8, H<sup>+</sup> form, 200-400 mesh. This solution was then dried and taken up in 0.18 M HCl and loaded on a second column containing Eichrom<sup>©</sup> Ln resin (50-100 mesh) to isolate Sm and Nd from the other REE. All reagents were distilled and the average total chemical blank measured at the MUN TIMS laboratory was less than 100 pg for Nd and therefore considered negligible. Thus no blank correction was performed

Samarium and Nd concentrations and the Nd isotopic composition was determined using a multi-collector Finnigan Mat 262 mass spectrometer in static for concentration determination, and dynamic mode for Nd isotopic composition determination. Instrumental mass fractionation of Sm and Nd isotopes was corrected using a Raleigh law relative to  $^{146}\text{Nd}/^{144}\text{Nd} = 0.7219$  and  $^{152}\text{Sm}/^{147}\text{Sm} = 1.783$ . The reported values were adjusted to the JNd-1 standard ( $^{143}\text{Nd}/^{144}\text{Nd} = 0.512115$ , Tanaka et al., 2000). During the course of this study JNd-1 yield a mean  $^{143}\text{Nd}/^{144}\text{Nd} = 0.512101 \pm 16$  (2SD, n=40). Five analyses of USGS whole rock reference material BRC-2 were run during the course of this study. Each analysis comprised a separate dissolution and thus provides the best estimate of the reproducibility of an individual whole rock analysis. The mean values of BCR-2 are as follows where the relative two standard deviations of the mean are given in percent in parenthesis;  $^{143}\text{Nd}/^{144}\text{Nd} = 0.512636 (0.0025\%)$ ;  $^{147}\text{Sm}/^{144}\text{Nd} = 0.1384 (0.25\%)$ ; Nd ppm=27.7 (0.7%); Sm = 6.34 (0.6%). These values are in excellent agreement with recent determinations made in other laboratories (eg., Razcek et al., 2001; Razcek et al., 2003; Schmitz et al., 2004; Weis et al., 2006). The analytical uncertainty given for Nd isotopic ratios is the in-run precision expressed as two standard error of the mean (2SE) and is typically <0.002%.

### **Zircon U-Th-Pb analytical methods**

Zircon U-Pb geochronology and scanning ion imaging was performed using a CAMECA IMS1280 large geometry ion microprobe at the Nordsim facility, NRM. Geochronological analyses follow routine protocols outlined by Whitehouse et al. (1999) and Whitehouse and Kamber (2005). A ca. 4.5 nA, -13 kV O<sub>2</sub><sup>-</sup> primary beam (imaged

aperture of 150  $\mu\text{m}$  corresponding to a spot diameter on the sample of ca. 15  $\mu\text{m}$ ) was used to generate +10 kV secondary ions which were admitted to the mass spectrometer and detected in a peak-hopping sequence using a single ion-counting electron multiplier. The mass spectrometer was operated at a mass resolution ( $M/\Delta M$ ) of 5400, sufficient to separate all species of interest from molecular interferences. Each analysis comprised a 90 second pre-sputter to remove the Au-coating and allow the secondary beam to stabilize, centering of the secondary beam in the field aperture, energy optimization in the 45 eV energy window, mass calibration adjustment using the  $^{90}\text{Zr}_2^{16}\text{O}$  peak, and 12 cycles through the species of interest. Groups of analyses were performed in fully automated sequences, regularly interspersing standard analyses with those of the sample zircon grains. Data reduction utilized an in-house developed suite of software. Pb-isotope ratios were corrected for common Pb estimated from measured  $^{204}\text{Pb}$  assuming the present-day terrestrial Pb isotope composition estimated from the model of Stacey and Kramers (1975); where the  $^{204}\text{Pb}$  count was statistically insignificant relative to the long-term background on the EM, no correction was applied. U/Pb ratios were calibrated using an empirical power-law relationship between  $^{206}\text{Pb}/^{238}\text{U}$  and  $^{238}\text{U}^{16}\text{O}_2/^{238}\text{U}$  assuming the 1065 Ma age of the 91500 zircon (Wiedenbeck et al., 1995). Age calculations assume the decay constant recommendations of Steiger and Jäger (1975) and utilize the routines of Isoplot-Ex (Ludwig, 2004).

### Zircon Lu-Hf analytical methods

Following SIMS analysis of the U-Pb-Th ages, zircons were analyzed for their Lu-Hf isotope composition at Memorial University of Newfoundland. Analyses were

done using a ThermoFinnigan Neptune MC-ICPMS coupled to a Geolas Pro 193 nm Ar-F excimer laser operating at 10Hz, 5 J/cm<sup>2</sup>, and a 50 um diameter spot size. The cup configuration, analytical methodology, and data reduction protocol are described in detail in Fisher et al. (2011b).

## REFERENCES

- Corfu, F., 1988, Differential response of U-Pb systems in coexisting accessory minerals, Winnipeg River Subprovince, Canadian Shield: implications for Archean crustal growth and stabilization: Contributions to Mineralogy & Petrology, v. 98, p.312–325.
- Fisher, C.M., McFarlane, C.R.M., Hanchar, J.M., Schmitz, M.D., Sylvester, P.J., Lam, R., and Longerich, H.P., 2011a, Sm-Nd isotope systematics by laser ablation-multicollector-inductively coupled plasma mass spectrometry: Methods and potential natural and synthetic reference materials: Chemical Geology, v. 284, p. 1-20.
- Fisher, C.M., Hanchar, J.M., Samson, S.D., Dhuime, B., Blichert-Toft, J., Vervoort, J.D., Lam, R., 2011b. Synthetic zircon doped with hafnium and rare earth elements: A reference material for in situ hafnium isotope analysis: Chemical Geology 286, 32-47.
- Goudie, D. J., Fisher, C.M., Hanchar, J.M., Crowley, J.L., & Ayers, J.C., 2014. Simultaneous in situ determination of U-Pb and Sm-Nd isotopes in monazite by laser ablation ICP-MS: Geochemistry, Geophysics, Geosystems, 15, pp. 2575-2600.
- Jackson, S.E., Longerich, H.P., Dunning, G.R., and Fryer, B.J., 1992, The application of laser-ablation microprobe- inductively coupled plasma - mass spectrometry (LAM-ICP-MS) to in situ trace-element determinations in minerals: Canadian Mineralogist, v. 30, p. 1049-1064.
- Kirkland, C.L., Whitehouse, M.J., and Slagstad, T., 2009, Fluid-assisted zircon and monazite growth within a shear zone: a case study from Finnmark, Arctic Norway: Contributions to Mineralogy & Petrology, v. 158, p. 637–657.
- McDonough, W.F., Sun, S.-S., 1995, Composition of the Earth: Chemical Geology, v. 120, p. 223-253.

- Mulcahy, S.R., King, R.L., and Vervoort, J.D., 2009, Lawsonite Lu-Hf geochronology: A new geochronometer for subduction zone processes: *Geology*, v. 37, p. 987-990.
- Paton, C., J. D. Woodhead, J. C. Hellstrom, J. M. Hergt, A. Greig, and R. Maas (2010), Improved laser ablation U-Pb zircon geochronology through robust downhole fractionation correction: *Geochem. Geophys. Geosyst.*, 11, Q0AA06.
- Paton, C., J. C. Hellstrom, B. Paul, J. D. Woodhead, and J. M. Hergt (2011), Iolite: Freeware for the visualisation and processing of mass spectrometric data: *J. Anal. At. Spectrom.* 26, 2508-2518, doi: 10.1039/c1ja10172b
- Raczek, I., Jochum, K.P., and Hofmann, A.W., 2003, Neodymium and strontium isotope data for USGS reference materials BCR-1, BCR-2, BHVO-1, BHVO-2, AGV-1, AGV-2, GSP-1, GSP-2 and eight MPI-DING reference glasses: *Geostandards Newsletter*, v. 27, p. 173-179.
- Schmitz, M.D., Vervoort, J.D., Bowring, S.A., and Patchett, P.J., 2004, Decoupling of the Lu-Hf and Sm-Nd isotope systems during the evolution of the granulitic lower crust beneath southern Africa: *Geology*, v. 32, p. 405-408.
- Tanaka, T., Togashi, S., Kamioka, H., Amakawa, H., Kagami, H., Hammoto, T., Yuhara, M., Orihashi, Y., Yoneda, S., Shimizu, H., Kunimaru, T., Takahashi, K., Yanagi, T., Nakano, T., Fujimaka, H., Shinjo, R., Asahara, Y., Tanimizu, M., and Dragusanu, C., 2000, JNDI-1: a neodymium isotopic reference in consistency with LaJolla neodymium: *Chemical Geology*, v. 168, p. 279-281.
- Weis, D., Kieffer, B., Maerschalk, C., Barling, J., de Jong, J., Williams, G.E., Hanano, D., Pretorius, W., Mattielli, N., Scoates, J.S., Goolaerts, A., Friedman, R.M., and Mahoney, J.B., 2006, High-precision isotopic characterization of USGS reference materials by TIMS and MC-ICPMS: *Geochemistry, Geophysics, and Geosystems*, v. 7, p. 1-30.
- Whitehouse, M. J., and Kamber, B. S., 2005, Assigning dates to thin gneissic veins in high-grade metamorphic terranes - a cautionary tale from Akilia, southwest Greenland: *Journal of Petrology*, v. 46, p. 291-318.
- Whitehouse, M.J., Kamber, B.S., and Moorbat, S., 1999, Age significance of U-Th-Pb zircon data from early Archaean rocks of west Greenland – a reassessment based on combined ion-microprobe and imaging studies: *Chemical Geology*, v. 160, p. 201-224.

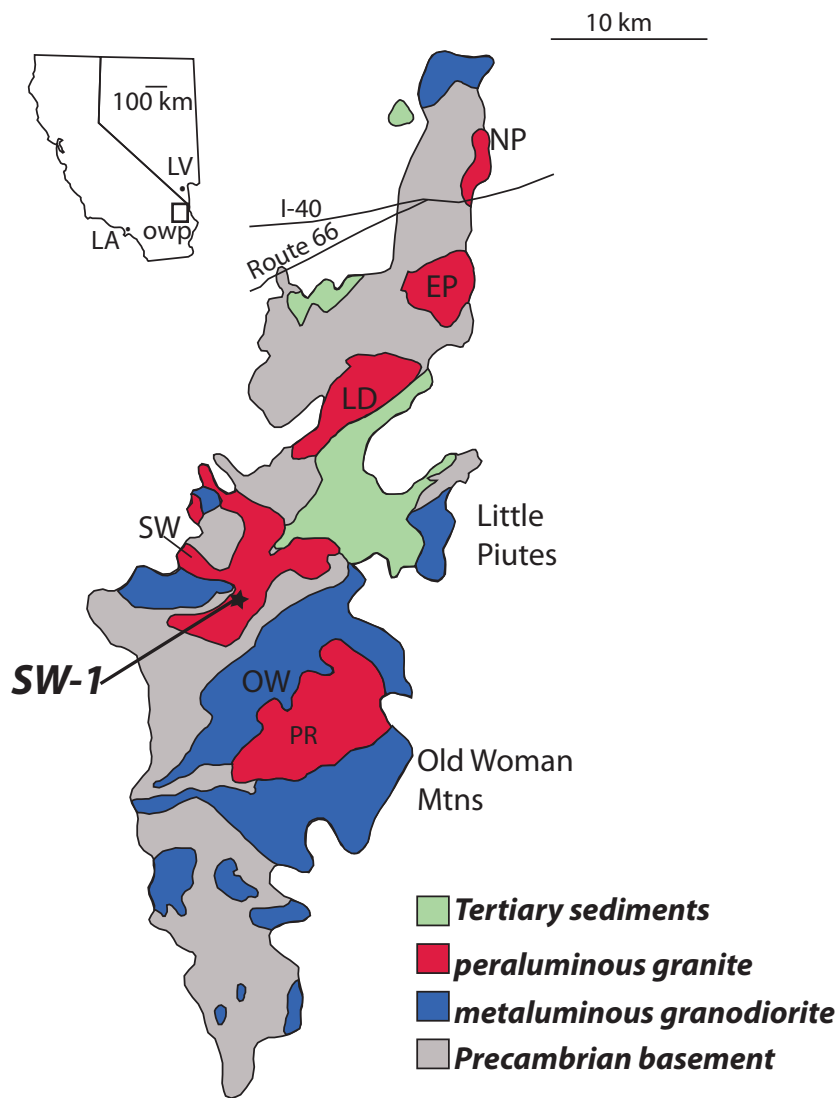


**Figure DR1.** Geologic map of the Late Cretaceous Old Woman-Puite Range batholith, southeastern California. Star denotes sample location of SW-1 discussed in this study. Modified after Foster et al., 1992. PR-Painted Rock pluton, OW-Old Woman pluton, SW- Sweetwater Wash pluton, LD-Lazy Daisy pluton, EP -East Puite pluton, NP-North Puite pluton.

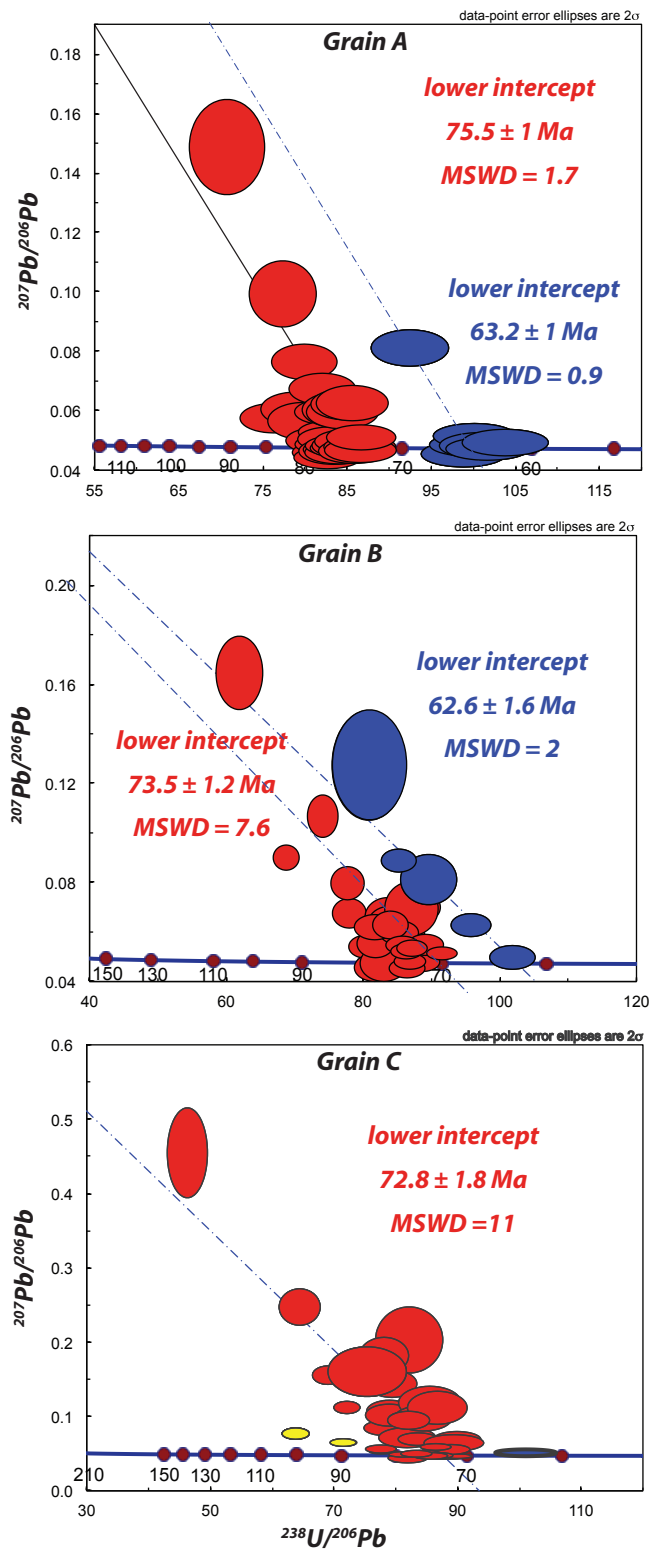


**Figure DR2.** Tera-Wasserburg plot of SW-1 monazite grains A, B, and C.

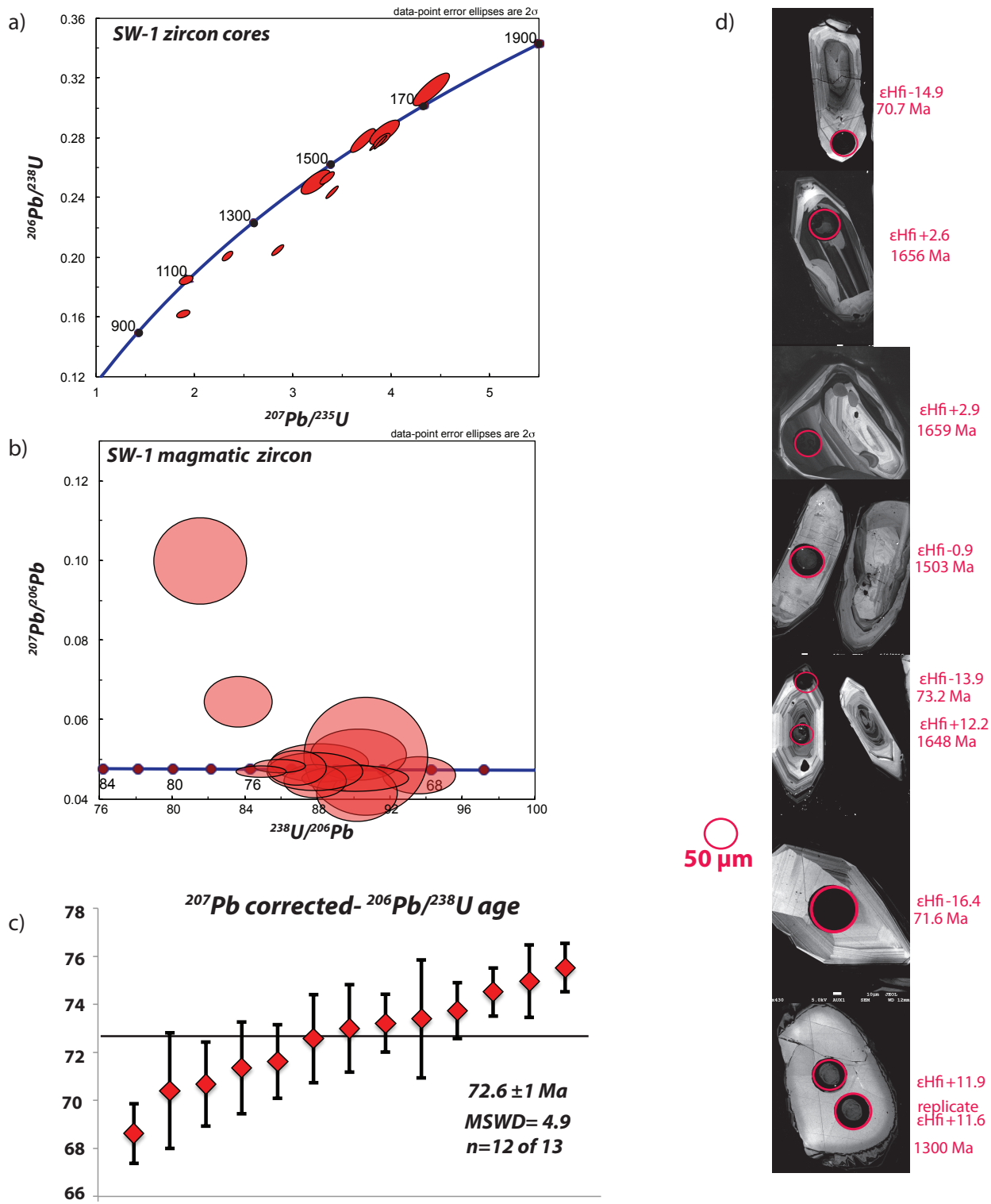


**Figure DR3.** U-Pb age data for SW-1 zircon samples. a) concordia plot of inherited zircon cores ; b) Tera-Wasserburg plot of magmatic zircon; c) weighted mean  $^{207}\text{Pb}$  corrected  $^{206}\text{Pb}/^{238}\text{U}$  ages of magmatic zircon; d) representative cathodoluminescence images (CL) of zircon crystals in sample SW-1, along with initial  $\epsilon\text{Hf}$  values calculated at the preferred age (U/Pb age for Cretaceous zircon; Pb/Pb age for Proterozoic zircon), laser spot size is 50μm in all images.

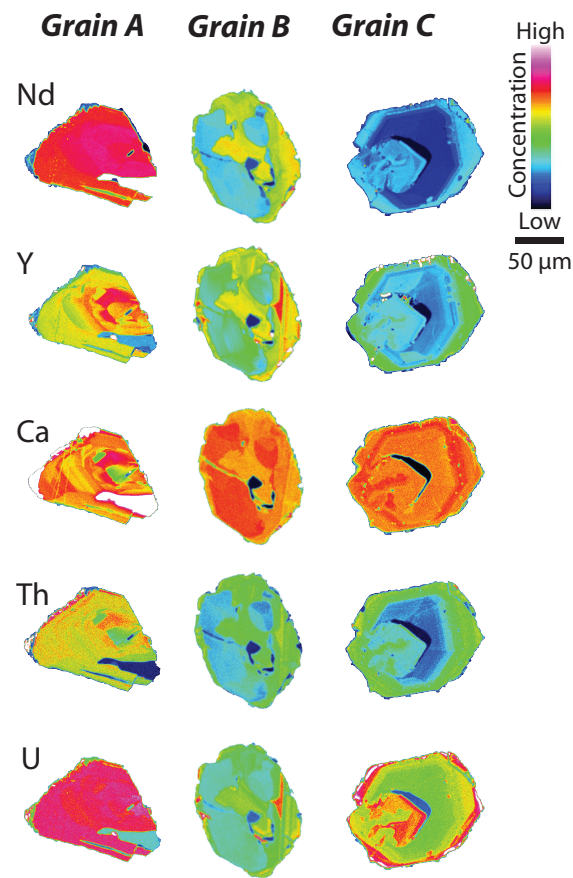


**Figure DR4.** Compositional (elemental) x-ray maps for the monazite grains A, B, and C

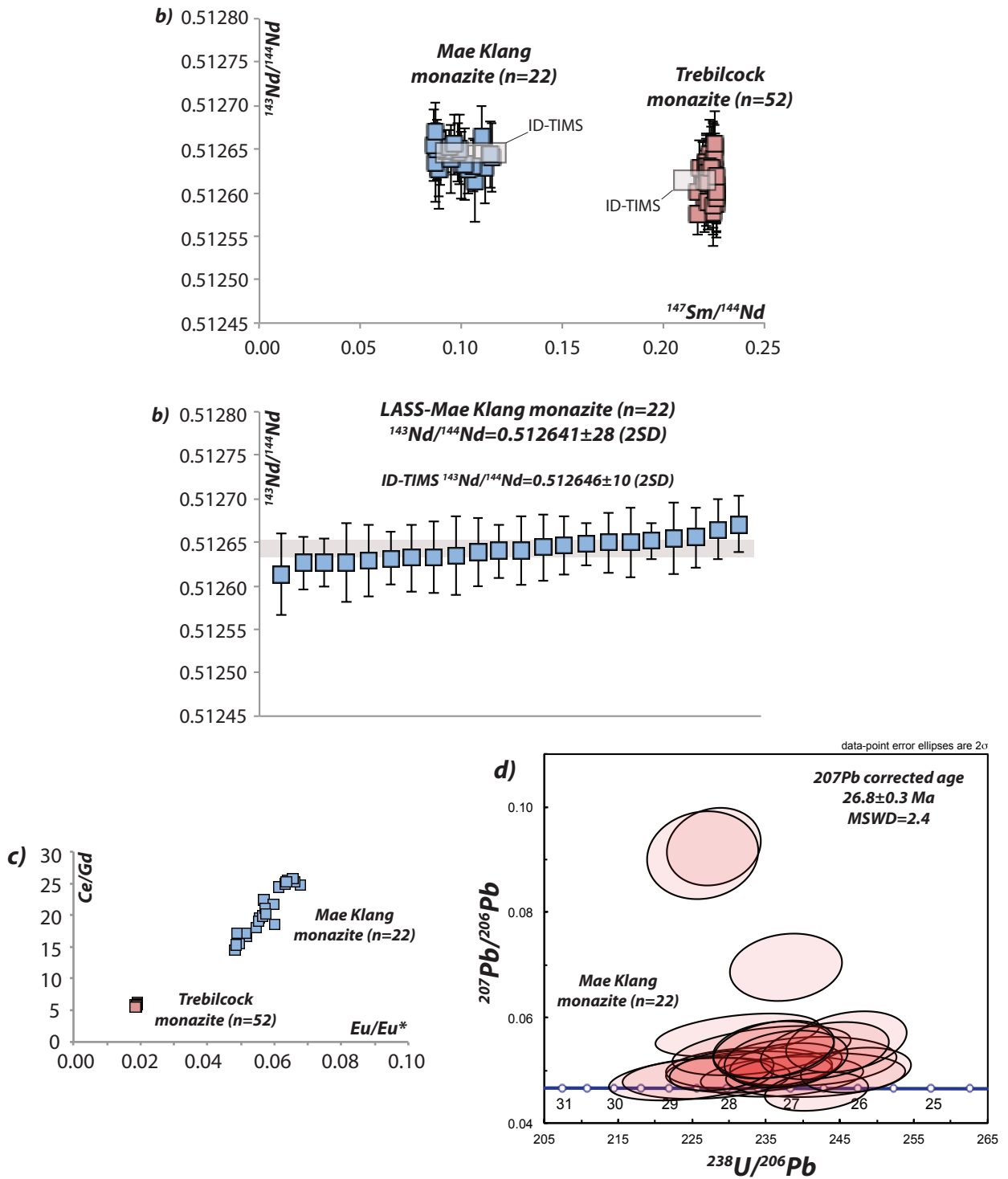


**Figure DR5.** a) Reproducibility of Mae Klang and Trebilcock monazite Nd-standards for  $^{143}\text{Nd}/^{144}\text{Nd}$  and  $^{147}\text{Sm}/^{144}\text{Nd}$  compared to ID-TIMS analyses (in grey box). Note that Trebilock analyses are self-normalized for  $^{143}\text{Nd}/^{144}\text{Nd}$ , but not for  $^{147}\text{Sm}/^{144}\text{Nd}$ . b) Reproducibility of  $^{143}\text{Nd}/^{144}\text{Nd}$  for the Mae Klang Nd-standard compared to ID-TIMS, note reproducibitly is ~0.5 epsilon units (2SD). c) Reproducibility of Mae Klang and Trebilcock monazite Nd-standards for Ce/Gd vs. Eu/Eu\*. d) Tera-Wasserburg diagram of concurrent U-Pb age results from the Mae Klang monazite; ID-TIMS age 26.8 Ma (Dunning et al., 1995)

Table OR1. Sm-Nd and U-Pb isotopic data for monazite grains A, B, and C

Sample	#Sm (V)	#U (V)	#Nd (V)	#Sr (V)	#Zr (V)	#La (V)	#Ce (V)	#Nd/Sm <sup>143</sup>	#U/Pb <sup>207</sup>	#Eu/Eu <sup>206</sup>	Ce/La	Origin/Location	Comments	#Sm/Sm <sup>143</sup>	#U/U <sup>235</sup>	#La/Sm <sup>143</sup>	#Ce/Ce <sup>143</sup>	#Nd/Nd <sup>143</sup>	#U/U <sup>238</sup>	#Eu/Eu <sup>206</sup>	Ce/La	Origin/Location	Comments	#Sm/Sm <sup>143</sup>	#U/U <sup>235</sup>	#La/Sm <sup>143</sup>	#Ce/Ce <sup>143</sup>	#Nd/Nd <sup>143</sup>	#U/U <sup>238</sup>	#Eu/Eu <sup>206</sup>	Ce/La	Origin/Location	Comments	#Sm/Sm <sup>143</sup>	#U/U <sup>235</sup>	#La/Sm <sup>143</sup>	#Ce/Ce <sup>143</sup>	#Nd/Nd <sup>143</sup>	#U/U <sup>238</sup>	#Eu/Eu <sup>206</sup>	Ce/La	Origin/Location	Comments							
Gran-A-01	1.41	0.51218645	0.000021	0.3848422	0.000019	0.0895	-32.22	0.45	-32.05	0.143	20.74	62	SW1-g1-02	0.0518	0.021	0.010	0.0002	0.062	95.7009	1.9881	0.0484	0.0016	0.259	0.00005	51	2	64	1	61	1	64.1	1.3	61.6	1.3	61.6	1.3	61.6	1.3	61.6	1.3	61.6	1.3	61.6	1.3	61.6	1.3	61.6	1.3	61.6	1.3
Gran-A-02	0.25	1.88	0.51218645	0.000031	0.3848422	0.000019	0.0897	-0.0005	-15.79	0.68	-14.12	0.132	20.74	62	SW1-g1-02	0.0518	0.021	0.010	0.0002	0.062	95.7009	1.9881	0.0484	0.0016	0.259	0.00005	51	2	64	1	61	1	64.1	1.3	61.6	1.3	61.6	1.3	61.6	1.3	61.6	1.3	61.6	1.3	61.6	1.3	61.6	1.3	61.6	1.3
Gran-A-03	0.25	1.88	0.51218645	0.000031	0.3848422	0.000019	0.0897	-0.0005	-15.79	0.68	-14.12	0.132	20.74	62	SW1-g1-02	0.0518	0.021	0.010	0.0002	0.062	95.7009	1.9881	0.0484	0.0016	0.259	0.00005	51	2	64	1	61	1	64.1	1.3	61.6	1.3	61.6	1.3	61.6	1.3	61.6	1.3	61.6	1.3	61.6	1.3	61.6	1.3	61.6	1.3
Gran-A-04	0.22	1.55	0.51218645	0.000042	0.3848407	0.000019	0.0946	0.0005	-16.04	0.82	-14.38	0.15	18.18	64	SW1-g1-04	0.0312	0.021	0.002	0.0002	0.007	82.4462	1.6111	0.0473	0.016	0.275	0.00005	53	3	78	1	77	1	77.8	1.6	76.6	1.6	76.6	1.6	76.6	1.6	76.6	1.6	76.6	1.6	76.6	1.6	76.6	1.6	76.6	1.6
Gran-A-05	0.24	1.77	0.51218645	0.000029	0.3848418	0.000019	0.0919	0.0018	-15.03	0.57	-13.36	0.196	19.63	64	SW1-g1-05	0.0840	0.021	0.010	0.002	-0.036	83.2640	1.6398	0.0516	0.017	0.340	0.00007	51	3	77	2	76	1	77.8	1.6	76.6	1.6	76.6	1.6	76.6	1.6	76.6	1.6	76.6	1.6	76.6	1.6	76.6	1.6		
Gran-A-06	0.24	1.43	0.51218645	0.000029	0.3848418	0.000019	0.0919	0.0018	-15.03	0.57	-13.36	0.196	19.63	64	SW1-g1-05	0.0840	0.021	0.010	0.002	-0.036	83.2640	1.6398	0.0516	0.017	0.340	0.00007	51	3	77	2	76	1	77.8	1.6	76.6	1.6	76.6	1.6	76.6	1.6	76.6	1.6	76.6	1.6	76.6	1.6	76.6	1.6		
Gran-A-07	0.18	1.57	0.51218645	0.000021	0.3848403	0.000019	0.0888	0.0005	-18.87	1.00	-17.20	0.143	20.72	64	SW1-g1-07	0.0786	0.021	0.010	0.002	0.011	84.5109	1.6077	0.0487	0.016	0.246	0.00007	51	3	76	1	75	1	75.7	1.6	75.7	1.6	75.7	1.6	75.7	1.6	75.7	1.6	75.7	1.6	75.7	1.6				
Gran-A-08	0.23	1.76	0.51218645	0.000021	0.3848402	0.000020	0.0889	0.0010	-15.40	0.74	-13.74	0.124	22.48	64	SW1-g1-09	0.0491	0.021	0.009	0.002	0.045	103.1122	2.0599	0.0495	0.018	0.283	0.00006	48	2	65	1	61	1	61.3	1.3	61.3	1.3	61.3	1.3	61.3	1.3	61.3	1.3	61.3	1.3	61.3	1.3				
Gran-A-09	0.20	1.20	0.51218645	0.000044	0.3848425	0.000020	0.0883	0.0012	-15.52	0.86	-13.84	0.195	21.13	64	SW1-g1-10	0.0983	0.021	0.010	0.002	0.114	84.4505	1.7477	0.0467	0.021	0.215	0.00007	53	4	76	2	75	1	74.6	1.6	74.6	1.6	74.6	1.6	74.6	1.6	74.6	1.6	74.6	1.6	74.6	1.6				
Gran-A-10	0.20	1.54	0.51218645	0.000044	0.3848425	0.000020	0.0883	0.0012	-15.52	0.86	-13.84	0.195	21.13	64	SW1-g1-10	0.0983	0.021	0.010	0.002	0.114	84.4505	1.7477	0.0467	0.021	0.215	0.00007	53	4	76	2	75	1	74.6	1.6	74.6	1.6	74.6	1.6	74.6	1.6	74.6	1.6	74.6	1.6						
Gran-A-11	0.23	1.24	0.51218645	0.000021	0.3848412	0.000019	0.0871	0.0013	-15.48	0.55	-13.81	0.141	21.69	64	SW1-g1-14	0.0795	0.021	0.010	0.002	0.108	82.6446	1.6051	0.0467	0.018	0.231	0.00008	53	3	76	1	75	1	74.2	1.6	74.2	1.6	74.2	1.6	74.2	1.6	74.2	1.6	74.2	1.6	74.2	1.6				
Gran-A-12	0.17	1.34	0.51218645	0.000028	0.3848412	0.000019	0.0871	0.0013	-15.48	0.55	-13.81	0.141	21.69	64	SW1-g1-14	0.0795	0.021	0.010	0.002	0.108	82.6446	1.6051	0.0467	0.018	0.231	0.00008	53	3	76	1	75	1	74.2	1.6	74.2	1.6	74.2	1.6	74.2	1.6	74.2	1.6	74.2	1.6	74.2	1.6				
Gran-A-13	0.17	1.34	0.51218645	0.000028	0.3848412	0.000019	0.0871	0.0013	-15.48	0.55	-13.81	0.141	21.69	64	SW1-g1-14	0.0795	0.021	0.010	0.002	0.108	82.6446	1.6051	0.0467	0.018	0.231	0.00008	53	3	76	1	75	1	74.2	1.6	74.2	1.6	74.2	1.6	74.2	1.6	74.2	1.6	74.2	1.6	74.2	1.6				
Gran-A-14	0.17	1.34	0.51218645	0.000028	0.3848412	0.000019	0.0871	0.0013	-15.48	0.55	-13.81	0.141	21.69	64	SW1-g1-14	0.0795	0.021	0.010	0.002	0.108	82.6446	1.6051	0.0467	0.018	0.231	0.00008	53	3	76	1	75	1	74.2	1.6	74.2	1.6	74.2	1.6	74.2	1.6	74.2	1.6	74.2	1.6						
Gran-A-15	0.18	1.35	0.51218645	0.000029	0.3848427	0.000019	0.0883	0.0005	-19.01	0.57	-17.14	0.142	20.95	64	SW1-g1-15	0.0467	0.021	0.009	0.002	0.089	101.7294	2.0130	0.0484	0.016	0.285	0.00006	50	4	76	1	75	1	74.2	1.6	74.2	1.6	74.2	1.6	74.2	1.6	74.2	1.6	74.2	1.6						
Gran-A-16	0.18	1.35	0.51218645	0.000029	0.3848427	0.000019	0.0883	0.0005	-19.01	0.57	-17.14	0.142	20.95	64	SW1-g1-15	0.0467	0.021	0.009	0.002	0.089	101.7294	2.0130	0.0484	0.016	0.285	0.00006	50	4	76	1	75	1	74.2	1.6	74.2	1.6	74.2	1.6	74.2	1.6	74.2	1.6	74.2	1.6						
Gran-A-17	0.2	1.62	0.51218645	0.000028	0.3848435	0.000019	0.0891	0.0005	-19.32	0.55	-17.40	0.140	20.51	38	SW1-g1-17	0.0749	0.021	0.010	0.002	0.097	81.4024	1.7942	0.0477	0.018	0.215	0.00008	53	3	77	2	74	1	74.2	1.6	74.2	1.6	74.2	1.6	74.2	1.6	74.2	1.6	74.2	1.6						
Gran-A-18	0.2	1.62	0.51218645	0.000028	0.3848435	0.000019	0.0891	0.0005	-19.32	0.55	-17.40	0.140	20.51	38	SW1-g1-17	0.0749	0.021	0.010	0.002	0.097	81.4024	1.7942	0.0477	0.018	0.215	0.00008	53	3	77	2	74	1	74.2	1.6	74.2	1.6	74.2	1.6	74.2	1.6	74.2	1.6								
Gran-A-19	0.18	1.23	0.51218645	0.000028	0.3848435	0.000019	0.0891	0.0005	-19.32	0.55	-17.40	0.140	20.51	38	SW1-g1-17	0.0749	0.021	0.010	0.002	0.097	81.4024	1.7942	0.0477	0.018	0.215	0.00008	53	3	77	2	74	1	74.2	1.6	74.2	1.6	74.2	1.6	74.2	1.6	74.2	1.6								
Gran-A-20	0.18	1.23	0.51218645	0.000028	0.3848435	0.000019	0.0891	0.0005	-19.32	0.55	-17.40	0.140	20.51	38	SW1-g1-17	0.0749	0.021	0.010	0.002	0.097	81.4024	1.7942	0.0477	0.018	0.215	0.00008	53	3	77	2	74	1	74.2	1.6	74.2	1.6	74.2	1.6	74.2	1.6	74.2	1.6								
Gran-A-21	0.17	1.23	0.51218645	0.000028	0.3848435	0.000019	0.0891	0.0005	-19.32	0.55	-17.40	0.140	20.51	38	SW1-g1-17	0.0749	0.021	0.010	0.002	0.097	81.4024	1.7942	0.0477	0.018	0.215	0.00008	53	3	77	2	74	1	74.2	1.6	74.2	1.6	74.2	1.6	74.2	1.6	74.2	1.6								
Gran-A-22	0.2	1.78	0.51218645	0.000028	0.3848435	0.000019	0.0891	0.0005	-19.32	0.55	-17.40	0.140	20.51	38	SW1-g1-17	0.0749	0.021	0.010	0.002	0.097	81.4024	1.7942	0.0477	0.018	0.215	0.00008	53	3	77	2	74	1	74.2	1.6	74.2	1.6	74.2	1.6	74.2	1.6	74.2	1.6								
Gran-A-23	0.2	1.78	0.51218645	0.000028	0.3848435	0.000019	0.0891	0.0005	-19.32	0.55	-17.40	0.140	20.51	38	SW1-g1-17	0.0749</td																																		

Table DR2. Lu-Hf and U-Pb isotope data for SW1 zircons

	$^{176}\text{Hf}^{177}\text{Hf}$	2SE	$^{176}\text{Lu}^{177}\text{Hf}$	2SE	$^{176}\text{Yb}^{177}\text{Hf}$	2SE	$^{176}\text{Hf}^{177}\text{Hf}$	2SE	$\epsilon\text{Hf}(t)$ <sup>†</sup>	2SE	$\epsilon\text{Hf}(73\text{Ma})$ <sup>†</sup>		$^{206}\text{Pb}^{204}\text{U}$	1SE	$^{206}\text{Pb}^{204}\text{U}$	1SE	$\rho_{\text{Hf}}$	$^{206}\text{Pb}^{204}\text{Pb}$	1SE	$^{206}\text{Pb}^{204}\text{Pb}$	age (Ma)	1SE	$^{206}\text{Pb}^{204}\text{U}$	1SE	$^{206}\text{Pb}^{204}\text{U}$	1SE	$^{207}\text{corr}$	age (Ma)	1SE	$\text{U}$ (ppm)	Th (ppm)	T/H
SW1_b	0.282369	0.000021	0.000493	0.00034	1.02792	0.000947	1.467237	0.000031	0.282369	-13.1	0.8	-	0.05624	11.78	0.0112	0.10946	0.03653	11.71	nd	291.4	55.6	6.4	71.6	0.9	72.6	0.9	120	106	0.89			
SW1_13	0.282317	0.000028	0.000472	0.00012	0.015219	0.000217	1.467264	0.000003	0.282316	-15.1	1.0	-	0.04717	12.79	0.0105	0.94	0.07354	0.03257	12.76	nd	336.6	46.8	5.9	67.4	0.6	68.6	0.6	132	66	0.50		
SW1_83	0.282320	0.000019	0.000251	0.00005	0.006833	0.000175	1.467236	0.000003	0.282320	-14.9	0.7	-	0.05708	15.04	0.0109	1.30	0.08622	0.03800	14.98	nd	357.3	56.4	8.3	69.8	0.9	70.7	0.9	66	49	0.75		
SW1_h	0.282319	0.000031	0.000729	0.00068	0.018138	0.001727	1.467273	0.000050	0.282318	-15.0	1.1	-	no data	no data	0.0106	1.81	no data	nd	nd	nd	nd	68.2	1.2	70.4	1.2	19	21	1.11				
SW1_76	0.282276	0.000030	0.000569	0.000013	0.016623	0.000338	1.467246	0.000043	0.282275	-16.4	1.1	-	0.06332	7.10	0.0111	1.01	0.14170	0.04142	7.03	nd	169.5	62.3	4.3	71.1	0.7	71.6	0.8	34	51	1.50		
SW1_j	0.282427	0.000021	0.001422	0.000134	0.034405	0.003241	1.467231	0.000039	0.282425	-11.1	0.8	-	0.05979	5.78	0.0110	1.35	0.23273	0.03936	5.62	nd	140.4	59.0	3.3	70.6	0.9	71.4	1.0	224	79	0.35		
SW1_74r	0.282347	0.000024	0.00138	0.00068	0.040932	0.001994	1.467247	0.000040	0.282346	-13.9	0.9	-	0.06203	6.27	0.0113	0.81	0.12907	0.03977	6.22	nd	153.9	61.1	3.7	72.5	0.6	73.2	0.6	103	128	1.24		
SW1_e	0.282378	0.000029	0.000651	0.000043	0.017668	0.001094	1.467250	0.000044	0.282377	-12.8	1.0	-	0.05367	11.44	0.0112	1.26	0.10986	0.03473	11.37	nd	291.8	53.1	5.9	71.8	0.9	73.0	0.9	109	56	0.51		
SW1_i	0.282324	0.000024	0.000638	0.000042	0.007443	0.000938	1.467251	0.000045	0.282312	-17.1	1.0	-	no data	no data	0.0110	nd	nd	nd	nd	nd	nd	nd	70.5	1.5	73.4	1.2	50	120	2.40			
SW1_132	0.282273	0.000033	0.000648	0.000024	0.008682	0.000550	1.467237	0.000050	0.282356	-16.5	1.2	-	0.07265	4.78	0.0115	0.77	0.18599	0.04590	4.48	nd	100.7	71.2	3.1	73.6	0.6	73.7	0.6	144	147	1.03		
SW1_130	0.282357	0.000021	0.001338	0.000041	0.023254	0.000715	1.467217	0.000041	0.282356	-13.5	0.8	-	0.07509	4.78	0.0116	0.67	0.17643	0.04688	4.65	nd	39.0	73.5	1.3	74.5	0.5	75.0	0.5	884	351	0.40		
SW1_107	0.282326	0.000038	0.001128	0.000039	0.029318	0.000545	1.467276	0.000075	0.282324	-14.6	1.3	-	0.08113	9.94	0.0117	0.99	0.10001	0.05014	8.89	nd	214.8	79.2	7.6	75.2	0.7	75.0	0.8	82	96	1.17		
SW1_134	0.282418	0.000023	0.000945	0.000015	0.030801	0.008282	1.467240	0.000035	0.282417	-11.4	0.8	-	0.07486	1.52	0.0118	0.66	0.14668	0.04615	1.37	nd	38.1	73.3	1.1	75.4	0.5	75.5	0.5	969	102	0.11		
SW1_72	0.282311	0.000031	0.000623	0.000143	0.018356	0.007299	1.467279	0.000044	0.282298	6.9	1.1	-15.2	1.91459	1.50	0.1846	0.67	0.4529	0.07524	1.34	1074.9	26.7	1086.2	10.0	109.1	40	26	0.66					
SW1_47c	0.282223	0.000030	0.000913	0.00016	0.023778	0.000241	1.467275	0.000051	0.282200	8.5	1.1	-18.3	2.33417	0.95	0.2008	0.66	0.61115	0.08433	0.69	1300.1	13.4	1222.7	6.8	117.4	116	51	0.44					
SW1_58	0.281820	0.000023	0.000609	0.000007	0.019337	0.000371	1.467275	0.000038	0.281805	-5.4	0.8	-32.6	1.88608	1.45	0.1620	0.66	0.45442	0.08446	1.29	1303.2	24.9	1076.2	9.7	967.6	56	67	1.19					
SW1_195	0.281844	0.000029	0.000650	0.000052	0.018807	0.001492	1.467278	0.000037	0.281825	-0.1	1.0	-31.7	3.23346	1.88	0.2502	1.32	0.70425	0.09372	1.33	1502.5	25.0	1465.2	14.7	1439.6	23	18	0.78					
SW1_25	0.281888	0.000034	0.000802	0.000025	0.026212	0.001139	1.467291	0.000054	0.281864	2.3	1.2	-30.1	3.34982	0.87	0.2529	0.68	0.77379	0.09660	0.55	1549.0	10.3	1492.7	6.8	1453.5	187	143	0.77					
SW1_d	0.282163	0.000025	0.000533	0.000035	0.013218	0.000998	1.467248	0.000040	0.282148	12.7	0.9	-20.4	3.71122	1.37	0.2781	1.15	0.83958	0.09680	0.74	1563.4	13.9	1573.8	11.0	1581.6	80	31	0.39					
SW1_j	0.281851	0.000021	0.000538	0.000057	0.014294	0.001453	1.467252	0.000037	0.281834	1.8	0.8	-31.5	1.27340	1.42	0.0948	1.26	0.88652	0.09739	0.66	1574.8	12.2	833.9	8.1	580.4	390	85	0.22					
SW1_g	0.282033	0.000034	0.000688	0.000018	0.017708	0.000401	1.467241	0.000033	0.282012	9.5	1.2	-25.0	3.93227	1.57	0.2836	1.16	0.73917	0.10057	1.05	1634.6	19.5	1620.3	12.8	1609.4	35	18	0.53					
SW1_33	0.282090	0.000030	0.001068	0.000027	0.031751	0.000529	1.467181	0.000044	0.282057	11.3	1.1	-23.0	2.84766	0.86	0.2046	0.72	0.83554	0.10095	0.47	1641.7	8.7	1368.2	6.5	1199.9	211	101	0.48					
SW1_61	0.281829	0.000029	0.000814	0.000028	0.025112	0.001273	1.467236	0.000041	0.281804	2.4	1.0	-32.2	3.84720	0.70	0.2759	0.68	0.96857	0.10115	0.18	1645.3	3.2	1602.7	5.7	1570.5	1244	689	0.55					
SW1_74c	0.282095	0.000031	0.000504	0.000032	0.015048	0.000942	1.467236	0.000045	0.282079	12.2	1.1	-22.8	3.40024	0.76	0.2434	0.69	0.91604	0.10130	0.31	1648.1	5.7	1504.5	6.0	1404.6	653	45	0.07					
SW1_18	0.281816	0.000029	0.000783	0.000014	0.026060	0.000238	1.467257	0.000052	0.281791	2.2	1.0	-32.7	3.90546	0.88	0.2783	0.68	0.76919	0.10174	0.56	1656.0	10.4	1614.4	7.1	1582.7	107	132	1.23					
SW1_81	0.281854	0.000027	0.001390	0.000032	0.036763	0.000670	1.467241	0.000032	0.281810	2.9	1.0	-31.4	3.89076	0.70	0.2770	0.68	0.96094	0.10189	0.19	1658.8	3.6	1611.8	5.7	1576.0	779	127	0.16					
SW1_164	0.281809	0.000023	0.000642	0.000011	0.012115	0.000276	1.467229	0.000039	0.281794	2.5	0.8	-32.9	4.40476	1.71	0.3123	1.42	0.83022	0.10229	0.95	1666.1	17.5	1713.2	14.2	1752.1	34	27	0.78					

<sup>†</sup>εHf is determined using the CHUR parameters of Bouvier et al. (2008)

**Table DR3. Whole rock major and trace element geochemistry.**

Analyte	SW-1	Unit	Detection Limit
SiO <sub>2</sub>	73.06	%	0.01
Al <sub>2</sub> O <sub>3</sub>	15.36	%	0.01
Fe <sub>2</sub> O <sub>3</sub> (T)	1.89	%	0.01
MnO	0.03	%	0.001
MgO	0.29	%	0.01
CaO	1.72	%	0.01
Na <sub>2</sub> O	3.76	%	0.01
K <sub>2</sub> O	3.93	%	0.01
TiO <sub>2</sub>	0.136	%	0.001
P <sub>2</sub> O <sub>5</sub>	0.06	%	0.01
LOI	0.43	%	
Total	<b>100.7</b>	%	0.01
Sc	3	ppm	1
Be	3	ppm	1
V	8	ppm	5
Cr	260	ppm	20
Co	28	ppm	1
Ni	120	ppm	20
Cu	10	ppm	10
Zn	50	ppm	30
Ga	20	ppm	1
Ge	1.5	ppm	0.5
As	< 5	ppm	5
Rb	131	ppm	1
Sr	474	ppm	2
Y	21.4	ppm	0.5
Zr	169	ppm	1
Nb	23	ppm	0.2
Mo	5	ppm	2
Ag	0.6	ppm	0.5
In	< 0.1	ppm	0.1
Sn	5	ppm	1
Sb	< 0.2	ppm	0.2
Cs	3.4	ppm	0.1
Ba	1483	ppm	3
La	37.6	ppm	0.05
Ce	72.9	ppm	0.05
Pr	7.93	ppm	0.01
Nd	28.7	ppm	0.05
Sm	5.33	ppm	0.01
Eu	0.924	ppm	0.005
Gd	3.89	ppm	0.01
Tb	0.63	ppm	0.01
Dy	3.87	ppm	0.01
Ho	0.8	ppm	0.01
Er	2.37	ppm	0.01
Tm	0.367	ppm	0.005
Yb	2.43	ppm	0.01
Lu	0.368	ppm	0.002
Hf	4.4	ppm	0.1
Ta	5.43	ppm	0.01
W	295	ppm	0.5
Tl	0.57	ppm	0.05
Pb	35	ppm	5
Bi	0.4	ppm	0.1
Th	13.6	ppm	0.05
U	2.17	ppm	0.01
Sm (ppm)	5.08		
Nd (ppm)	28.86		
<sup>147</sup> Sm/ <sup>144</sup> Nd	0.1064		
<sup>143</sup> Nd/ <sup>144</sup> Nd	0.511778		
2SE	0.000007		
$\epsilon_{\text{Nd}_{73\text{Ma}}}$ <sup>1</sup>	-15.8		
Eu/Eu*	0.61		
Ce/Gd	18.7		

<sup>1</sup> $\epsilon_{\text{Nd}}$  values calculated using CHUR values of Bouvier et al., (2008).

**Table DR4. Sm-Nd and U-Pb isotope results for Trebilcock monazite**

Analysis	$^{147}\text{Sm}$ (V)	$^{146}\text{Nd}$ (V)	measured $^{143}\text{Nd}/^{144}\text{Nd}$	2SE	measured $^{145}\text{Nd}/^{144}\text{Nd}$	2SE	$^{147}\text{Sm}/^{144}\text{Nd}$	2SE	Eu/Eu*	Ce/Gd
Treb_1	0.47	1.39	0.512581	0.000027	0.348436	0.000016	0.2248	0.0003	0.019	5.913
Treb_2	0.43	1.30	0.512544	0.000033	0.348382	0.000014	0.2250	0.0003	0.019	5.934
Treb_3	0.44	1.33	0.512578	0.000034	0.348398	0.000014	0.2240	0.0003	0.019	6.039
Treb_4	0.42	1.29	0.512506	0.000038	0.348403	0.000020	0.2243	0.0003	0.019	6.044
Treb_5	0.40	1.23	0.512563	0.000034	0.348413	0.000019	0.2232	0.0004	0.019	6.116
Treb_6	0.41	1.26	0.512548	0.000034	0.348383	0.000016	0.2239	0.0002	0.019	5.992
Treb_7	0.40	1.22	0.512570	0.000025	0.348384	0.000015	0.2237	0.0003	0.019	6.038
Treb_8	0.41	1.27	0.512533	0.000029	0.348435	0.000020	0.2202	0.0003	0.019	6.164
Treb_9	0.42	1.29	0.512562	0.000043	0.348425	0.000018	0.2230	0.0003	0.019	5.996
Treb_10	0.40	1.24	0.512540	0.000031	0.348430	0.000021	0.2195	0.0003	0.019	6.150
Treb_11	0.41	1.28	0.512544	0.000021	0.348447	0.000018	0.2192	0.0002	0.019	6.136
Treb_12	0.37	1.13	0.512555	0.000036	0.348434	0.000017	0.2212	0.0004	0.019	6.042
Treb_13	0.57	1.73	0.512547	0.000033	0.348459	0.000027	0.2221	0.0001	0.019	5.893
Treb_14	0.41	1.25	0.512527	0.000032	0.348425	0.000020	0.2218	0.0005	0.019	5.985
Treb_15	0.39	1.18	0.512538	0.000032	0.348439	0.000023	0.2204	0.0004	0.019	6.030
Treb_16	0.37	1.14	0.512564	0.000034	0.348442	0.000018	0.2205	0.0004	0.019	6.023
Treb_17	0.41	1.25	0.512535	0.000044	0.348430	0.000013	0.2210	0.0002	0.019	5.883
Treb_18	0.35	1.09	0.512515	0.000031	0.348463	0.000015	0.2201	0.0005	0.019	6.023
Treb_19	0.35	1.10	0.512530	0.000028	0.348449	0.000016	0.2164	0.0003	0.019	6.156
Treb_20	0.35	1.07	0.512543	0.000034	0.348459	0.000024	0.2201	0.0004	0.019	5.940
Treb_21	0.32	1.00	0.512556	0.000032	0.348433	0.000018	0.2189	0.0005	0.019	6.004
Treb_22	0.36	1.11	0.512505	0.000024	0.348439	0.000015	0.2169	0.0004	0.019	5.996
Treb_23	0.37	1.15	0.512558	0.000031	0.348441	0.000017	0.2172	0.0002	0.019	5.973
Treb_1	0.53	1.59	0.512526	0.000045	0.348445	0.000022	0.2257	0.0002	0.019	5.657
Treb_2	0.46	1.43	0.512528	0.000030	0.348452	0.000015	0.2223	0.0003	0.019	5.899
Treb_3	0.51	1.56	0.512569	0.000040	0.348437	0.000020	0.2224	0.0003	0.019	5.870
Treb_4	0.48	1.47	0.512555	0.000028	0.348437	0.000018	0.2222	0.0003	0.019	5.891
Treb_5	0.50	1.53	0.512561	0.000030	0.348440	0.000018	0.2212	0.0004	0.019	5.913
Treb_6	0.46	1.39	0.512520	0.000035	0.348444	0.000020	0.2245	0.0005	0.019	5.777
Treb_7	0.47	1.43	0.512564	0.000042	0.348428	0.000019	0.2244	0.0003	0.019	5.769
Treb_8	0.45	1.38	0.512553	0.000031	0.348445	0.000014	0.2247	0.0004	0.019	5.703
Treb_9	0.47	1.42	0.512544	0.000039	0.348437	0.000018	0.2247	0.0005	0.019	5.716
Treb_10	0.41	1.25	0.512528	0.000027	0.348420	0.000022	0.2252	0.0004	0.019	5.641
Treb_11	0.47	1.43	0.512539	0.000035	0.348433	0.000015	0.2255	0.0005	0.019	5.632
Treb_12	0.46	1.39	0.512535	0.000022	0.348427	0.000013	0.2259	0.0003	0.019	5.541
Treb_13	0.43	1.30	0.512512	0.000038	0.348443	0.000021	0.2258	0.0004	0.019	5.581
Treb_14	0.42	1.31	0.512514	0.000031	0.348427	0.000017	0.2214	0.0004	0.019	5.869
Treb_15	0.44	1.37	0.512550	0.000029	0.348436	0.000018	0.2225	0.0003	0.019	5.725
Treb_16	0.46	1.42	0.512564	0.000030	0.348425	0.000017	0.2251	0.0004	0.019	5.625
Treb_17	0.42	1.31	0.512556	0.000027	0.348439	0.000020	0.2210	0.0003	0.019	5.864
Treb_18	0.46	1.43	0.512555	0.000027	0.348430	0.000013	0.2232	0.0007	0.019	5.737
Treb_19	0.43	1.33	0.512556	0.000030	0.348451	0.000016	0.2216	0.0003	0.019	5.819
Treb_20	0.41	1.26	0.512541	0.000031	0.348439	0.000020	0.2214	0.0004	0.019	5.804
Treb_21	0.45	1.36	0.512523	0.000032	0.348431	0.000018	0.2258	0.0005	0.019	5.631
Treb_22	0.44	1.37	0.512549	0.000037	0.348424	0.000014	0.2214	0.0004	0.019	5.783
Treb_23	0.47	1.42	0.512510	0.000033	0.348452	0.000017	0.2243	0.0013	0.019	5.570
Treb_24	0.55	1.71	0.512537	0.000033	0.348453	0.000018	0.2214	0.0001	0.019	5.769
Treb_25	0.42	1.28	0.512554	0.000038	0.348441	0.000019	0.2231	0.0011	0.019	5.710
Treb_26	0.46	1.41	0.512518	0.000038	0.348434	0.000016	0.2257	0.0005	0.019	5.578
Treb_27	0.46	1.42	0.512582	0.000037	0.348432	0.000016	0.2254	0.0003	0.018	5.567
Treb_28	0.44	1.34	0.512527	0.000037	0.348440	0.000016	0.2255	0.0004	0.019	5.582
Treb_29	0.47	1.43	0.512545	0.000033	0.348435	0.000011	0.2260	0.0003	0.018	5.514

Table DR4. Sm-Nd and U-Pb isotope results for Mae Klang monazite

Analysis	$\Delta m^2_{\text{Sv}}$		$\Delta m^2_{\text{Lw}}$		$\Delta m^2_{\text{Lw}} + \Delta m^2_{\text{Sv}}$		$\Delta m^2_{\text{Lw}} - \Delta m^2_{\text{Sv}}$		$\Delta m^2_{\text{Lw}}$		$\Delta m^2_{\text{Sv}}$		$\Delta m^2_{\text{Lw}} + \Delta m^2_{\text{Sv}}$		$\Delta m^2_{\text{Lw}} - \Delta m^2_{\text{Sv}}$		$\Delta m^2_{\text{Lw}}$		$\Delta m^2_{\text{Sv}}$		$\Delta m^2_{\text{Lw}} + \Delta m^2_{\text{Sv}}$		$\Delta m^2_{\text{Lw}} - \Delta m^2_{\text{Sv}}$		$\Delta m^2_{\text{Lw}}$		$\Delta m^2_{\text{Sv}}$				
	Sign	Value	Sign	Value	Sign	Value	Sign	Value	Sign	Value	Sign	Value	Sign	Value	Sign	Value	Sign	Value	Sign	Value	Sign	Value	Sign	Value	Sign	Value	Sign	Value	Sign	Value	
2d-Apr																															
Thur_1	0.15	1.18	0.252640	0.00001	0.344935	0.00001	0.093	0.2	0.6	0.9	0.055	25.310	Thur_2	0.09	0.002	0.0043	0.0002	0.072	232.56	9.1	0.0495	0.0032	0.00005	0.0013	28.7	2.3	2.7	1.1	0.0000	0.0000	
Thur_2	0.18	1.12	0.326263	0.00003	0.344932	0.00003	0.196	0.07	0.7	1.4	0.049	17.140	Thur_3	0.09	0.002	0.0043	0.0002	0.018	232.56	9.16	0.0503	0.0032	0.00005	0.0013	29.3	2.3	2.7	1.1	0.0000	0.0000	
Thur_3	0.15	1.13	0.326244	0.00003	0.344928	0.00003	0.142	0.07	0.7	0.9	0.049	15.300	Thur_4	0.033	0.002	0.0043	0.0002	0.100	230.95	9.07	0.0506	0.0033	0.00005	0.0014	29.0	2.4	2.7	1.1	0.0000	0.0000	
Thur_4	0.15	1.13	0.326244	0.00003	0.344928	0.00003	0.142	0.07	0.7	0.9	0.049	15.300	Thur_5	0.030	0.002	0.0043	0.0002	0.192	240.38	9.2	0.0516	0.0038	0.00005	0.0012	29.4	2.6	2.8	1.1	0.0000	0.0000	
Thur_5	0.15	1.13	0.326244	0.00003	0.344931	0.00003	0.106	0.01	0.8	0.7	0.050	18.550	Thur_6	0.030	0.002	0.0043	0.0002	0.017	234.94	9.1	0.0516	0.0038	0.00005	0.0012	29.4	2.6	2.8	1.1	0.0000	0.0000	
Thur_6	0.15	1.13	0.326244	0.00003	0.344931	0.00003	0.088	0.01	0.6	0.6	0.049	24.350	Thur_7	0.030	0.002	0.0043	0.0002	0.017	234.94	9.87	0.0536	0.0038	0.00005	0.0014	29.3	2.4	2.7	1.1	0.0000	0.0000	
Thur_7	0.15	1.13	0.326244	0.00003	0.344931	0.00003	0.112	0.007	0.8	0.6	0.049	15.520	Thur_8	0.029	0.002	0.0043	0.0002	0.002	218.24	9.72	0.0542	0.0033	0.00005	0.0017	28.4	2.3	2.6	1.1	0.0000	0.0000	
Thur_8	0.12	1.29	0.252629	0.00002	0.344932	0.00002	0.080	0.007	0.8	0.6	0.049	15.520	Thur_9	0.028	0.002	0.0043	0.0002	0.002	245.35	9.32	0.0549	0.0034	0.00005	0.0019	27.9	2.3	2.6	1.1	0.0000	0.0000	
Thur_9	0.18	1.2	0.326247	0.00003	0.344902	0.00003	0.083	0.007	0.7	1.0	0.055	19.060	Thur_10	0.028	0.002	0.0043	0.0002	0.007	235.00	9.6	0.0560	0.0034	0.00005	0.0020	27.9	2.3	2.6	1.1	0.0000	0.0000	
2d-Apr																															
Thur_1	0.24	1.59	0.526262	0.00002	0.344935	0.00009	0.102	-0.01	0.1	0.6	0.055	17.940	Thur_2	0.057	0.004	0.0044	0.0001	0.175	277.79	5.19	0.0592	0.006	0.00005	0.0015	55.5	3.6	28.2	0.7	27.2	0.6	
Thur_2	0.25	1.69	0.526262	0.00002	0.344944	0.00009	0.104	0.014	0.6	0.7	0.051	17.740	Thur_3	0.029	0.002	0.0044	0.0002	0.038	217.53	6.21	0.0511	0.0033	0.00005	0.0012	55.6	3.7	27.6	0.7	0.6	0.0000	
Thur_3	0.22	1.69	0.526262	0.00002	0.344944	0.00009	0.104	0.014	0.6	0.7	0.051	17.740	Thur_4	0.030	0.002	0.0044	0.0002	0.031	228.83	5.76	0.0498	0.0031	0.00005	0.0014	59.7	1.8	28.1	0.7	27.9	0.6	
Thur_4	0.22	1.30	0.326264	0.00003	0.344945	0.00003	0.146	-0.007	0.2	0.8	0.051	14.400	Thur_5	0.030	0.002	0.0044	0.0002	0.031	228.83	5.76	0.0498	0.0031	0.00005	0.0014	59.7	1.8	28.1	0.7	27.9	0.6	
Thur_5	0.22	1.39	0.326213	0.00003	0.344945	0.00003	0.146	-0.007	0.2	0.8	0.051	14.400	Thur_6	0.026	0.002	0.0044	0.0001	0.039	245.65	5.72	0.0499	0.0033	0.00005	0.0013	55.3	1.5	26.6	0.6	26.0	0.6	
Thur_6	0.22	1.39	0.326213	0.00003	0.344945	0.00003	0.146	-0.007	0.2	0.8	0.051	14.400	Thur_7	0.026	0.002	0.0044	0.0001	0.039	245.65	5.72	0.0499	0.0033	0.00005	0.0013	55.3	1.5	26.6	0.6	26.0	0.6	
Thur_7	0.20	1.44	0.326263	0.00002	0.344941	0.00007	0.099	0.006	0.4	0.4	1.1	0.057	21.030	Thur_8	0.031	0.002	0.0044	0.0002	0.0051	235.00	6.35	0.067	0.0038	0.00004	0.0019	30.2	2.4	27.3	0.7	27.3	0.7
Thur_8	0.19	1.19	0.326247	0.00003	0.344941	0.00002	0.090	0.003	0.5	0.5	1.0	0.056	21.030	Thur_9	0.031	0.002	0.0044	0.0002	0.0056	242.72	7.07	0.0636	0.0034	0.00004	0.0017	30.3	2.5	26.8	0.8	26.8	0.8
Thur_9	0.17	1.31	0.326262	0.00002	0.344942	0.00002	0.087	-0.001	0.1	0.6	0.058	24.730	Thur_10	0.037	0.003	0.0044	0.0002	0.0197	237.53	6.21	0.0634	0.0052	0.00004	0.0014	36.9	2.1	27.1	0.7	27.0	0.7	
Thur_10	0.17	1.31	0.326262	0.00002	0.344942	0.00002	0.087	-0.001	0.1	0.6	0.058	24.730	Thur_11	0.037	0.003	0.0044	0.0002	0.0197	237.53	6.21	0.0634	0.0052	0.00004	0.0014	36.9	2.1	27.1	0.7	27.0	0.7	
Thur_11	0.12	1.19	0.326264	0.00003	0.344945	0.00008	0.076	0.004	0.4	0.7	1.1	0.053	24.940	Thur_12	0.031	0.002	0.0044	0.0002	0.0057	235.00	6.67	0.0585	0.0045	0.00005	0.0016	31.3	2.5	27.8	0.7	27.4	0.7

mean 0.512641  
2SD 0.000028

— 1 —